

Effect of vacuum-induced coherence on single- and two-photon absorption in a four-level Y-type atomic system

B. P. Hou,^{1,2} S. J. Wang,^{2,3,*} W. L. Yu,⁴ and W. L. Sun¹

¹*Department of Physics, Sichuan Normal University, Chengdu 610068, People's Republic of China*

²*Institute of Physics, Southwest Jiaotong University, Chengdu 610031, People's Republic of China*

³*Department of Physics, Sichuan University, Chengdu 610064, People's Republic of China*

⁴*Chengdu University of Information Technology, Chengdu 610041, People's Republic of China*

(Received 2 September 2003; published 7 May 2004)

When a four-level Y-type atom with two highest nearly degenerate lying levels interacts with the same vacuum radiation field, its excited levels have vacuum-induced coherence due to the quantum interference between the spontaneous decay channels. We consider the effects of the vacuum-induced coherence on the electromagnetically induced transparency against single- and two-photon absorption in the atomic system. We find that the vacuum-induced coherence can lead to probe gain without incoherent pumping. On the other hand, the coherence can suppress the two-photon transparency, even in some cases where it can enhance the two-photon absorption. Another important result is the finding of the crucial role played by the relative phase between the probe and coupling fields: the two-photon transparency and the probe gain spectra can be modulated by this phase.

DOI: 10.1103/PhysRevA.69.053805

PACS number(s): 42.50.Gy, 42.50.Hz

I. INTRODUCTION

It is well known that an absorbing atomic medium driven by a strong coupling field may be transparent for a weak probe laser. This phenomenon, which is termed as electromagnetically induced transparency (EIT), has been studied in all kinds of three-level atomic configurations including V, Λ , and ladder schemes [1]. When the probe and coupling fields are resonant with their corresponding atomic transitions, the atomic medium displays perfect EIT for the probe field. Meanwhile two-photon absorption in the system may be enhanced. Agarwal and Harshawardhan considered a control laser to couple an intermediate state of the atom in the ladder configuration with another higher-excited state in order to form two interfering two-photon excitation paths among the dressed-state transitions and to create interference [2]. We call its configuration Y scheme. The two-photon absorption in this four-level Y-type atom can be suppressed or enhanced due to the destructive or constructive interference. Gao *et al.* reported an experimental observation of the electromagnetically induced inhibition of two-photon absorption in sodium atoms [3]. Wang *et al.* presented an experiment of electromagnetically induced two-photon transparency in ⁸⁵Rb atoms [4]. Xu *et al.* [5] investigated one- and two-photon transparencies for the isotopes ⁸⁵Rb and ⁸⁷Rb. Subsequently, Yan *et al.* reported an experimental observation of the transparency against single- and two-photon absorptions in the Λ -type four-level atom [6].

When the two highest-lying levels of the four-level Y-type atom are nearly degenerate and coupled by the same vacuum radiation field to the intermediate state, the system can create a vacuum-induced coherence (VIC) due to the

quantum interference between the two spontaneous decay channels. VIC leads to many remarkable phenomena such as the modification of absorption and dispersion properties of atomic systems [7–9], gain without inversion [10–12], and spontaneous emission and absorption spectra [13–15]. When considering the VIC effect, the probe gain with or without inversion [11,12] and spontaneous emission spectra [15] can be related to the relative phase between the probe and coupling fields.

The control of the two-photon absorption using quantum interference and the related coherence mechanism are of importance in the two-photon lasing, the pulse propagation [2,3], and the two-photon entanglement in quantum information processing [16,17]. Most of the previous work related to VIC was focused on the single-photon case. In the present paper we shall investigate the effects of the VIC on the two-photon absorption, which shows that the VIC is an important means to control the two-photon absorption. In addition, we also investigate the one-photon case corresponding to the upper transition in the two-photon excitation path. In the presence of the VIC in the four-level Y-type atom, we found some important phenomena in the system contrast to the conventional three-level V-type atom. The dependence of the single- and two-photon absorption spectra on the relative phase between the probe and control fields is also discussed. Our paper is organized as follows. In Sec. II we describe the model and present the density-matrix equations of motion for the system. In Sec. III we discuss the effects of VIC on the single- and two-photon absorption properties. The phase dependence of the absorption profiles is discussed in Sec. IV, and the conclusion is presented in Sec. V.

II. MODEL AND EQUATIONS

A four-level Y-type atom is shown in Fig. 1. The two-photon transition in the atom under consideration is induced

*Corresponding author. Email address: sjwang@home.swjtu.edu.cn

by a pump laser with frequency w_2 and Rabi frequency $G_2 = \vec{\mu}_{32} \cdot \vec{\epsilon}_2 / \hbar$ driving $|3\rangle \rightarrow |2\rangle$, and by a probe laser with frequency w_1 and Rabi frequency $G_1 = \vec{\mu}_{21} \cdot \vec{\epsilon}_1 / \hbar$ driving $|2\rangle \rightarrow |1\rangle$. We assume that Rabi frequency G_2 is a real parameter throughout the paper. A coupling laser with frequency w and Rabi frequency $G = \vec{\mu}_{24} \cdot \vec{\epsilon} / \hbar$ is applied on the transition $|2\rangle \rightarrow |4\rangle$ to produce dynamically induced coherence for the single- and two-photon transparencies. $2\gamma_1$ and 2γ are the spontaneous decay rates from levels $|1\rangle$ and $|4\rangle$ to level $|2\rangle$, respectively, and $2\gamma_2$ corresponds to the decay rate from $|2\rangle$ to $|3\rangle$. In the interaction picture the density-matrix equations of motion in the rotating-wave approximations can be written as

$$\begin{aligned} \frac{d\rho_{11}}{dt} &= -2\gamma_1\rho_{11} - (iG_1\rho_{12} + \eta\rho_{41} + \text{H.c.}), \\ \frac{d\rho_{33}}{dt} &= 2\gamma_2\rho_{22} + (iG_2\rho_{23} + \text{H.c.}), \\ \frac{d\rho_{44}}{dt} &= -2\gamma\rho_{44} - (iG\rho_{42} + \eta\rho_{41} + \text{H.c.}), \\ \frac{d\rho_{12}}{dt} &= -(\gamma_1 + \gamma_2 + i\Delta_1)\rho_{12} - iG_1^*\rho_{11} - iG_2\rho_{13} - iG^*\rho_{14} \\ &\quad + iG_1^*\rho_{22} - \eta\rho_{42}, \\ \frac{d\rho_{13}}{dt} &= -(\gamma_1 + i\Delta_1 + i\Delta_2)\rho_{13} - iG_2^*\rho_{12} + iG_1^*\rho_{23} - \eta\rho_{43}, \\ \frac{d\rho_{14}}{dt} &= -(\gamma_1 + \gamma + i\Delta_1 - i\Delta)\rho_{14} - iG\rho_{12} + iG_1^*\rho_{24} \\ &\quad - \eta(\rho_{11} + \rho_{44}), \\ \frac{d\rho_{23}}{dt} &= -(\gamma_2 + i\Delta_2)\rho_{23} + iG_1\rho_{13} - iG_2^*\rho_{22} + iG_2^*\rho_{33} + iG\rho_{43}, \\ \frac{d\rho_{24}}{dt} &= -(\gamma + \gamma_2 - i\Delta)\rho_{24} + iG_1\rho_{14} - iG\rho_{22} + iG_2^*\rho_{34} + iG\rho_{44} \\ &\quad - \eta\rho_{21}, \\ \frac{d\rho_{34}}{dt} &= -(\gamma - i\Delta_2 - i\Delta)\rho_{34} - iG\rho_{32} + iG_2\rho_{24} - \eta\rho_{31}. \end{aligned} \quad (1)$$

The above density matrix elements obey the conditions $\rho_{11} + \rho_{22} + \rho_{33} + \rho_{44} = 1$ and $\rho_{ij} = \rho_{ji}^*$. The detunings of the probe, pumping, and coupling lasers in Eq. (1) are defined as $\Delta_1 = w_{12} - w_1$, $\Delta_2 = w_{23} - w_2$, and $\Delta = w_{42} - w$, respectively. The terms with $\eta = p\sqrt{\gamma_1\gamma}$ in Eq. (1) represent the VIC effect resulted from the cross-coupling between two decay paths $|1\rangle \rightarrow |2\rangle$ and $|4\rangle \rightarrow |2\rangle$. The parameter p is defined as $p = \vec{\mu}_{12} \cdot \vec{\mu}_{42} / (|\vec{\mu}_{12}| |\vec{\mu}_{42}|) = \cos \theta$ where θ is the angle between dipole matrix elements $\vec{\mu}_{12}$ and $\vec{\mu}_{42}$. If the matrix elements $\vec{\mu}_{12}$ and $\vec{\mu}_{42}$ are orthogonal to each other, i.e., $p=0$, the VIC

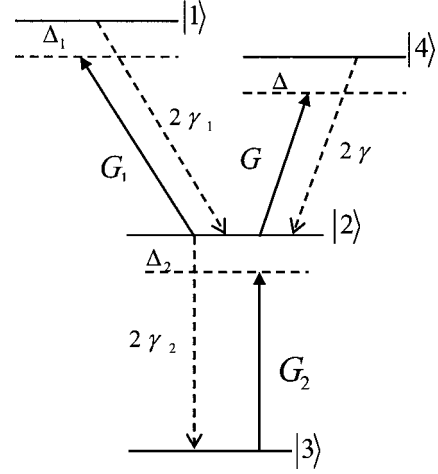


FIG. 1. The energy scheme of the four-level Y-type atom.

disappears. So the existence of the VIC depends on the non-orthogonality of the matrix elements $\vec{\mu}_{12}$ and $\vec{\mu}_{42}$. Here we only consider the case where the probe laser only acts on the transition $|1\rangle \leftrightarrow |2\rangle$ and the coupling laser only on the transition $|4\rangle \leftrightarrow |2\rangle$, so that the polarization direction of the probe field is perpendicular to $\vec{\mu}_{42}$ and that of the coupling field perpendicular to $\vec{\mu}_{12}$, i.e., $\vec{\epsilon}_1 \cdot \vec{\mu}_{42} = 0$ and $\vec{\epsilon} \cdot \vec{\mu}_{12} = 0$. Then the Rabi frequencies G_1 and G are associated with the angle θ as follows: $G_1 = G_{10} \sin \theta$ and $G = G_0 \sin \theta$ with $G_{10} = |\vec{\mu}_{12}| |\vec{\epsilon}_1| / \hbar$ and $G_0 = |\vec{\mu}_{24}| |\vec{\epsilon}| / \hbar$. To gain the remarkable VIC effect on optical properties of the system we assume that the excited levels are nearly degenerate, i.e., $w_{14} \approx 0$ or else the terms with η and accompanied by an exponential factor $\exp(\pm w_{14}t)$, which are not shown here, have been averaged out [8,11,12].

In the conventional treatment where the behavior of the system only relies on the amplitudes and detunings of the external coherent fields but not on their phases, the Rabi frequencies G_1 and G are treated as real parameters. However, in our case, the system is sensitive to the phases of the probe and coupling fields due to the existence of VIC. We should treat the Rabi frequencies G_1 and G as complex parameters: $G_1 = g_1 e^{i\phi_1}$ and $G = g e^{i\phi}$ where ϕ_1 and ϕ are the phases of the probe and coupling fields, respectively. Let $\sigma_{ii} = \rho_{ii}$, $\sigma_{12} = \rho_{12} e^{i\phi_1}$, $\sigma_{42} = \rho_{42} e^{i\phi}$, $\sigma_{13} = \rho_{13} e^{i\phi_1}$, $\sigma_{43} = \rho_{43} e^{i\phi}$, $\sigma_{14} = \rho_{14} e^{i\Phi}$, and $\eta_\Phi = \eta \exp(i\Phi)$ with $\Phi = \phi_1 - \phi$ being the relative phase between the probe and control fields. The re-defined matrix element σ_{ij} ($i, j = 1, 2, 3, 4$) obeys the same differential equations (1) except replacing G_1 , G , and η by g_1 , g , and η_Φ , respectively.

The single-photon absorption behavior for the probe laser in the four-level Y-type atom can be described by the imaginary part of σ_{12} . The two-photon absorption strengths can be measured by the population distribution in the excited state $|1\rangle$, i.e., σ_{11} . We extend our discussion for the single- and two-photon cases under the two-photon resonance conditions $\Delta_1 + \Delta_2 = 0$ and $\Delta = 0$. The two-photon absorption minimum magnitude is independent of the value of Δ , but its minimum point is determined by the probe detuning Δ_1 [2]. The suppression of the single- and two-photon absorption induced by the external coherent field G can be understood by the

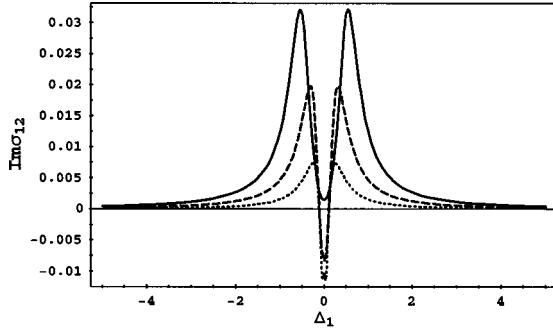


FIG. 2. The probe absorption $\text{Im} \sigma_{12}$ as a function of the probe detuning Δ_1 with $\gamma = \gamma_1 = 0.1$, $\gamma_2 = 0.3$, $g_0 = 0.5$, $g_{10} = g_2 = 0.1$, $\Phi = 0$ and different θ : $\theta = \pi/2$ (no VIC) (solid curve), $\theta = \pi/6$ (dashed curve), $\theta = \pi/18$ (dotted curve).

dressed states created by the coupling field: $|+\rangle = (1/\sqrt{2}) \times (|2\rangle + |4\rangle)$ and $|-\rangle = (1/\sqrt{2})(|2\rangle - |4\rangle)$ with the corresponding eigenvalues $E_+ = G$ and $E_- = -G$. The transparency against one-photon absorption corresponding to the transition $|2\rangle \rightarrow |1\rangle$ is induced by the interference between two channels: $|+\rangle \rightarrow |1\rangle$ and $|-\rangle \rightarrow |1\rangle$, and suppression of two-photon absorption for the transition $|3\rangle \rightarrow |2\rangle \rightarrow |1\rangle$ is induced by the interference between two paths: $|3\rangle \rightarrow |+\rangle \rightarrow |1\rangle$ and $|3\rangle \rightarrow |-\rangle \rightarrow |1\rangle$.

III. VIC-DEPENDENT ABSORPTION PROPERTIES

The steady-state behavior in the four-level Y-type atom can be described by setting $d\sigma_{ij}/dt = 0$. We describe the single- and two-photon absorption behaviors numerically by $\text{Im}(\sigma_{12})$ and σ_{11} , respectively. We plot the $\text{Im}(\sigma_{12})$ and σ_{11} versus the probe detuning Δ_1 in Figs. 2 and 3 with the relations $g = g_0 \sin \theta$, $g_1 = g_{10} \sin \theta$, $\eta_\Phi = p \sqrt{\gamma} \gamma_1 e^{i\Phi}$, and the parameter values $\gamma_1 = \gamma = 0.1$, $\gamma_2 = 0.3$, $g_0 = 0.5$, $g_{10} = g_2 = 0.1$, and $\Phi = 0$. When the atomic system is driven resonantly by the coupling field G , both single- and two-photon transparencies appear, which are exhibited by the solid curves in Figs. 2 and 3, respectively.

In the following we consider the effects of the VIC on the single- and two-photon absorption. From the dashed curve

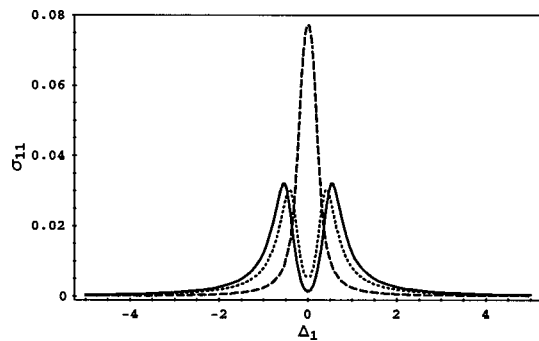


FIG. 3. The two-photon absorption σ_{11} as a function of the probe detuning Δ_1 with different θ : $\theta = \pi/2$ (no VIC) (solid curve), $\theta = \pi/6$ (dashed curve), $\theta = \pi/3$ (dotted curve). Other parameters are the same as those in Fig. 2.

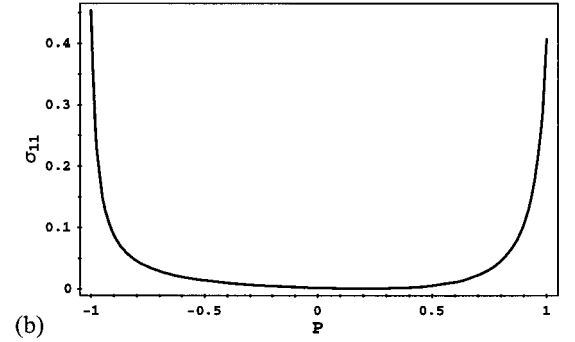
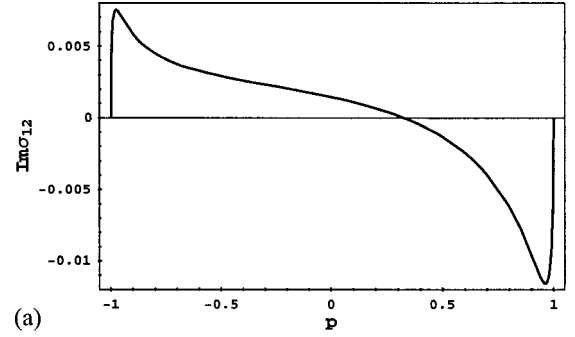


FIG. 4. The probe absorption $\text{Im} \sigma_{12}$ (a) and two-photon absorption σ_{11} (b) as the functions of p with $\Delta_1 = 0$. Other parameters are the same as those in Fig. 2.

with $\theta = \pi/6$ and the dotted curve with $\theta = \pi/18$ in Fig. 2, we see that the VIC can lead to the probe gain without incoherent pumping, and that the maximum gain with $\theta = \pi/18$ is larger than that with $\theta = \pi/6$. In the presence of VIC, the gain profile where the maximum gain appears at the probe resonant point, is different from that for the conventional V-type three-level atom where the probe gain spectral is symmetric with respect to the probe resonant point and vanishes at this resonant point [8,10]. This difference is due to the existence of the pump field G_2 driving the transition $|3\rangle \rightarrow |2\rangle$ in the four-level Y-type system.

In Fig. 3, it is seen from the dashed curve that the VIC enhances the two-photon absorption up to $\sigma_{11} = 0.077$ with $\theta = \pi/6$ ($\sigma_{11} = 0.048$ without control field, i.e., $G = 0$, which is not shown here). If $\theta = \pi/3$ as shown by the dotted curve in Fig. 3 we can see that the VIC suppresses the two-photon transparency by comparing with the solid curve.

To deeply investigate the effects of the VIC on the single- and two-photon absorption, we plot the single- and two-photon absorption versus p at the probe resonant point $\Delta_1 = 0$ in Fig. 4. Figure 4(a) shows that the single-photon absorption curve increases drastically with p in the regions $-1 < p < -0.976$ and $0.963 < p < 1$, but decreases monotonically with p from $p = -0.976$ to $p = 0.963$. It can be seen that the probe gain appears only when $0.328 < p < 1$ and reaches the maximum value at about the point $p = 0.963$. The dependence of the two-photon absorption on the VIC is exhibited in Fig. 4(b) by setting $\Delta_1 = 0$. The absorption spectrum against p looks like a concave, and the two-photon absorption minimum $\sigma_{11} = 3.32 \times 10^{-4}$ under the condition $\Delta_1 = 0$ appears at $p = 0.199$. From a comparison of pairs of plots as

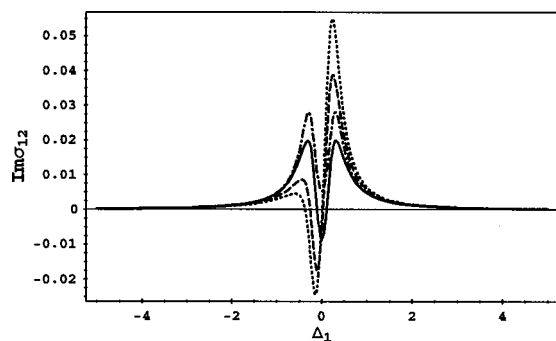


FIG. 5. The probe absorption $\text{Im} \sigma_{12}$ as a function of the probe detuning Δ_1 with $\theta = \pi/6$ and different Φ : $\Phi = 0$ (solid curve), $\Phi = \pi/6$ (dashed curve), $\Phi = \pi/3$ (dotted curve), $\Phi = \pi$ (dashed-dotted curve). Other parameters are the same as those in Fig. 2.

in Fig. 4 with different Rabi frequencies of the coupling laser (not given here), we can conclude that the oscillating magnitudes of the absorption curves in Fig. 4 become smaller and their crossing points in Fig. 4(a) are close to the resonant point as increasing Rabi frequencies of the coupling laser. This is due to the fact that contribution of the quantum interference from the increasing coherent field becomes dominant compared with that from VIC. When the coupling laser becomes stronger, the one- and two-photon absorption reduces on the resonant point, which is one of the factors leading to the movement of the crossing point close to the resonant point. The spectra in Fig. 4 display neither odd nor even symmetry between the positive and negative values of p . This can be understood as follows: the parameter p appears in part of terms, not all of the terms on the right-hand side of Eq. (1), which leads to that the matrix elements $\text{Im}(\sigma_{12})$ or σ_{11} contain both even and odd orders of p , such as zero order, one order, and higher orders of p (this is verified by their analytical expressions up to two orders of p), implying that the $\text{Im}(\sigma_{12})$ and σ_{11} are neither odd functions nor even functions of p and the spectra in Fig. 4 display neither odd nor even symmetries.

IV. PHASE-DEPENDENT ABSORPTION PROPERTIES

In the following we shall discuss that the one-photon absorption property is dependent on the phases of the probe and control fields due to the existence of the VIC. We plot the single-photon absorption versus probe detuning with given values of relative phase Φ in Fig. 5 where the other parameters are same as those in Fig. 2. It is seen that the maximal gain value in the case of $\Phi = \pi/6$, shown by the dashed curve in Fig. 5, becomes two times larger than that displayed by the solid curve without considering the relative phase, and that it is three times larger as $\Phi = \pi/3$ from the dotted curve. The gain profiles shown by the dashed and dotted curves become asymmetric and the maximal gain amplitudes move to the left near the resonant point due to the relative phase. From the dashed-dotted curve, we can see that the gain disappears for $\Phi = \pi$. The single-photon absorption profiles with $\Phi = \pi/2$ (solid line) and $\Phi = 3\pi/2$ (dashed line) in Fig. 6(a) show that they are symmetric about the resonant

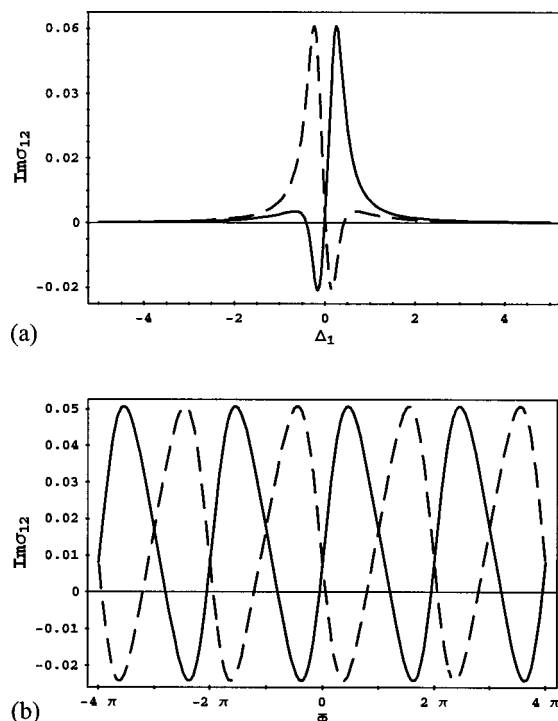


FIG. 6. (a) The probe absorption $\text{Im} \sigma_{12}$ as a function of the probe detuning Δ_1 with $\theta = \pi/6$ and different Φ : $\Phi = \pi/2$ (solid line), $\Phi = 3\pi/2$ (dashed line). (b) The probe absorption $\text{Im} \sigma_{12}$ as a function of the relative phase Φ with $\theta = \pi/6$ and different Δ_1 : $\Delta_1 = 0.162$ (solid line), $\Delta_1 = -0.162$ (dashed line). Other parameters are the same as those in Fig. 2.

point. Figure 6(b) shows the dependence of the single-photon absorption on the relative phase Φ at $\Delta_1 = 0.162$ (solid line) and $\Delta_1 = -0.162$ (dashed line). It is seen that the absorption profiles are periodic with the period of π and the maximum gain relies on the different detunings and different relative phases.

The two-photon absorption profiles in the presence of the relative phase Φ display similar behavior to that of the single-photon absorption. From the dashed curve in Fig. 7 with $\Phi = \pi/6$, we can see that the relative phase slightly shifts the minimum of the two-photon absorption to the left side and makes the minimum become smaller than that in the

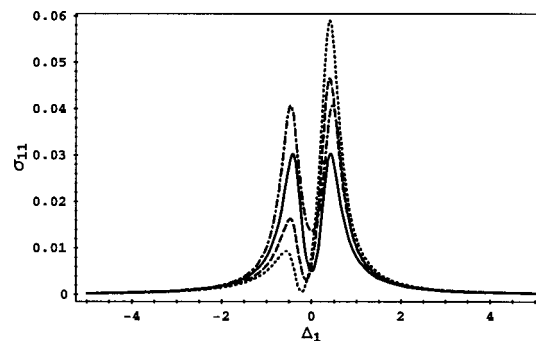


FIG. 7. The two-photon absorption σ_{11} as a function of the probe detuning Δ_1 with $\theta = \pi/3$ and different Φ : $\Phi = 0$ (solid curve), $\Phi = \pi/6$ (dashed curve), $\Phi = \pi/3$ (dotted curve), $\Phi = \pi$ (dashed-dotted curve). Other parameters are the same as those in Fig. 2.

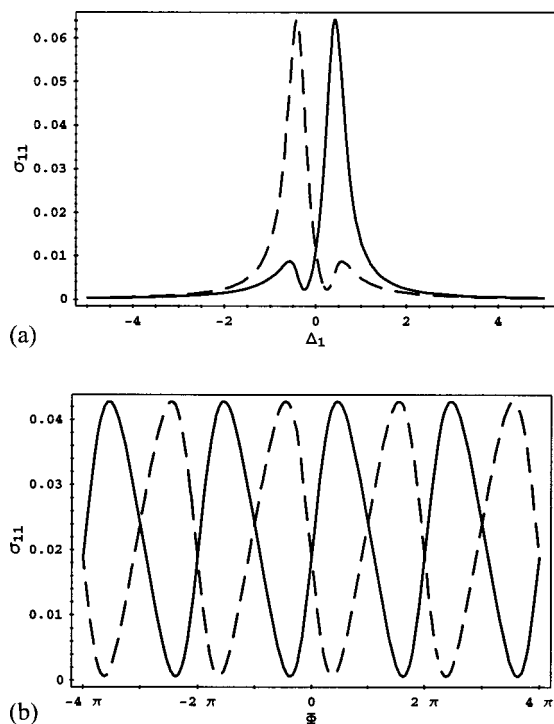


FIG. 8. (a) The two-photon absorption σ_{11} as a function of the probe detuning Δ_1 with $\theta = \pi/3$ and different Φ : $\Phi = \pi/2$ (solid line), $\Phi = 3\pi/2$ (dashed line). (b) The two-photon absorption σ_{11} as a function of the relative phase Φ with $\theta = \pi/3$ and different Δ_1 : $\Delta_1 = 0.25$ (solid line), $\Delta_1 = -0.25$ (dashed line). Other parameters are the same as those in Fig. 2.

absence of the relative phase. When $\Phi = \pi/3$, shown by the dotted curve in Fig. 7, the minimum becomes smaller than that in the case of $\Phi = \pi/6$. The two-photon absorption profile with $\Phi = \pi$, shown by the dashed-dotted curve in Fig. 7, is like that in Fig. 5 in the absence of the relative phase but the minimum becomes larger. Like Fig. 6(a), the two-photon absorption profile for $\Phi = \pi/2$ [solid line, see Fig. 8(a)], is symmetric with that in the case of $\Phi = 3\pi/2$ (dashed line). The modulation of the relative phase Φ on the two-photon absorption at $\Delta_1 = 0.25$ (solid line) and $\Delta_1 = -0.25$ (dashed line), shown in Fig. 8(b), is also similar to the case of single photon in Fig. 6(b). They also oscillate with the period π .

The above results are related to the experiment reported by Xia *et al.* [18]. The three-peak structure of the fluorescent intensity in their experiment can only be resulted from the presence of the two-step one-photon channels. This implies that there must be a near-resonant intermediate level (the singlet state) between the ground state and the two upper lying states [19]. Thus the atomic configuration in the present paper is similar to the level scheme of their experiment. Additionally, the two highest-lying states are used by a pair of mixed levels of the singlet and triplet states in sodium dimer, their superposition coefficients are determined just by tuning the frequency of the driving field [18]. Then the two highest-lying states are close to each other, and the dot products of the dipole matrix elements between the two highest-lying states and the intermediate level are determined not only by the dipole matrix elements between the singlet state and the intermediate singlet state but also by the superposition coefficients in the mixed levels [20]. Therefore the VIC parameter p can be nonzero by tuning the driving field.

V. CONCLUSIONS

In conclusion, we have investigated the electromagnetically induced one- and two-photon transparencies without or with VIC in the four-level Y-type atom. In the case of single-photon absorption the VIC can induce the probe gain around the probe resonant point, but it suppresses the two-photon transparency in the case of two-photon absorption. Due to the existence of VIC, the single- and two-photon absorption profiles are quite sensitive to the relative phase between the probe and coupling lasers: the two-photon transparency spectra and the probe gain can be modulated to different regions just by changing the relative phase.

ACKNOWLEDGMENTS

This work was supported in part by the National Natural Science Foundation of China under Grants Nos. 10175029 and 10375039, the Doctoral Education Fund of Education Ministry and the Research Fund of Nuclear Theory Center of HIRFL of China, and by the Education Foundation of Sichuan Province, China under Grant No. 2003A093, the Science and Technology Foundation of Sichuan Province, China under Grant No. 02GY029-189.

[1] K.-J. Boller, A. Imamolu, and S. E. Harris, *Phys. Rev. Lett.* **66**, 2593 (1991); S. E. Harris, *Phys. Today* **50**(7), 36 (1997).
 [2] G. S. Agarwal and W. Harshawardhan, *Phys. Rev. Lett.* **77**, 1039 (1996).
 [3] Jin-Yue Gao, Su-Hui Yang, Dong Wang, Xin-Zhen Guo, Kai-Xin Chen, Yun Jiang, and Bin Zhao, *Phys. Rev. A* **61**, 023401 (2000).
 [4] D. Wang, J. Y. Gao, J. H. Xu, G. C. La Rocca, and F. Bassani, *Europhys. Lett.* **54**, 456 (2001).
 [5] J. H. Xu, G. C. La Rocca, F. Bassani, D. Wang, and J. Y. Gao, *Opt. Commun.* **216**, 157 (2003).

[6] Min Yan, Edward G. Rickey, and Yifu-Zhu, *Phys. Rev. A* **64**, 043807 (2001).
 [7] Sunish Menon and G. S. Agarwal, *Phys. Rev. A* **57**, 4014 (1998).
 [8] Emmanuel Paspalakis, Shang-Qing Gong, and Peter L. Knight, *Opt. Commun.* **152**, 293 (1998).
 [9] Sunish Menon and G. S. Agarwal, *Phys. Rev. A* **61**, 013807 (2000).
 [10] Peng Zhou and S. Swain, *Phys. Rev. Lett.* **78**, 832 (1997).
 [11] Jin-Hui Wu and Jin-Yue Gao, *Phys. Rev. A* **65**, 063807 (2002); Wei-Hua Xu, Jin-Hui Wu, and Jin-Yue Gao, *ibid.* **66**,

- 063812 (2002).
- [12] Jin-Hui Wu, Zheng-Lin Yu, and Jin-Yue Gao, *Opt. Commun.* **211**, 257 (2002).
- [13] Peng Zhou and S. Swain, *Phys. Rev. Lett.* **77** 3995 (1996); Shi-Yao Zhu, *Phys. Rev. A* **52**, 710 (1995); Peng Zhou and S. Swain, *ibid.* **56**, 3011 (1997); Shi-Yao Zhu, Hong Chen, and Hu Huang, *Phys. Rev. Lett.* **79**, 205 (1997).
- [14] S. Y. Zhu and M. O. Scully, *Phys. Rev. Lett.* **76**, 388 (1996); Fu-li Li and Shi-Yao Zhu, *Phys. Rev. A* **59**, 2330 (1999); Hwang Lee, Pavel Polynkin, Marlan O. Scully, and Shi-Yao Zhu, *ibid.* **55**, 4454 (1997); P. R. Berman, *ibid.* **58**, 4886 (1998).
- [15] E. Paspalakis and P. L. Knight, *Phys. Rev. Lett.* **81**, 293 (1998); Fazal Ghafoor, Shi-Yao Zhu, and M. Suhail Zubairy, *Phys. Rev. A* **62**, 013811 (2000).
- [16] David Petrosyan and Gershon Kurizki, *Phys. Rev. A* **64**, 023810 (2001).
- [17] M. Paternostro and M. S. Kim, *Phys. Rev. A* **67**, 023811 (2003).
- [18] H. R. Xia, C. Y. Ye, and S. Y. Zhu, *Phys. Rev. Lett.* **77**, 1032 (1996).
- [19] J. Wang, H. M. Wiseman, and Z. Ficek, *Phys. Rev. A* **62**, 013818 (2000).
- [20] Anil. K. Patnaik and G. S. Agarwal, *J. Mod. Opt.* **45**, 2131 (1998).